Original paper

Crystal structure of undersubstituted Sb-rich vikingite Vik_{40}, $Ag_{2.85}Pb_{12.35}(Bi_{9.52}Sb_{1.27})_{\Sigma=10.80}S_{30}$: site population and comparison with structure of vikingite Vik_{50}, $Ag_{3.5}Pb_{11.0}Bi_{11.5}S_{30}$

Richard PAŽOUT[1,*], Michal DUŠEK[2]

[1] *University of Chemistry and Technology, Technická 5, 166 28 Prague 1, Czech Republic; richard.pazout@vscht.cz*
[2] *Institute of Physics of the Czech Academy of Sciences, Cukrovarnická 10/112, Prague, Czech Republic*
[*] *Corresponding author*

Crystal structure of Sb-rich vikingite with lillianite substitution percentage L% below 50% from Kutná Hora ore district, Czech Republic, was solved and refined from single-crystal diffraction data to determine the site populations of metal sites concerning a) the decreasing "lillianite" substitution $2\,Pb^{2+} = Ag^{+} + Bi^{3+}$; b) Sb content not known in vikingite from other localities throughout the world. Vikingite is monoclinic, *C*2/*m*, with $a = 13.5394(10)$, $b = 4.0992(3)$, $c = 25.506(3)$ Å, $\beta = 95.597(8)°$, $V = 1408.9(2)$ Å^3, $Z = 1$, $D_c = 7.0412$ g/cm^3. The structural formula derived from the refinement is $Ag_{2.85}Pb_{12.35}(Bi_{9.52}Sb_{1.27})_{\Sigma=10.80}S_{30}$, corresponding to $Vik_{40.0}$. The structure of vikingite is composed of thinner slabs (^{4}L) of four octahedra *Me*2–*Me*1–*Me*1–*Me*2 and thicker slabs (^{7}L) of seven octahedra *Me*4–*Me*5–*Me*6–*Me*7–*Me*6–*Me*5–*Me*4 separated by Pb atoms *Me*3 in trigonal prismatic coordination. The refinement showed differences between the structures of Vik_{40} and the previously published structure of Vik_{50}. The drop of L% below 50 % shows most profoundly in the marginal octahedral site *Me*2 of the thinner ^{4}L slabs, which becomes a Bi–Pb–Ag site with 28.6% of silver next to 50% of Bi and 21.4% of Pb. The central *Me*1 site from ^{4}L slabs which is almost a pure Bi site in Vik_{50} (0.97 Bi + 0.3 Ag) becomes a Bi-Pb site with minor Sb (0.54 Bi + 0.06 Sb + 0.40 Pb) in Vik_{40}. The Sb for Bi substitution was found to take place in the semimarginal site *Me*5 (0.74 Bi + 0.26 Sb) in the thicker ^{7}L slabs, which is a pure Bi site in Sb-free Vik_{50}. Another important change against Vik_{50} occurs in central octahedral site *Me*6 (pure Pb site in Vik_{50}), which becomes – despite the decrease in Bi content with decreasing L% – a Pb–Bi mix site. The correctness of the refined structural model was verified and the occupancies of mixed sites were fine-tuned employing charge distribution calculations in program ECoN21. In Vik_{40} weighted average bond lengths R_{AV} of the marginal sites *Me*2 and *Me*4 and of the central site *Me*1 are significantly larger than in Vik_{50}, reflecting the lower Ag content and the presence of Pb, while the Bi site *Me*5, which is partly substituted by Sb and the site *Me*6 with minor Bi at the expense of Pb exhibit adequately shortened R_{AV} values.

Keywords: vikingite, structure, site populations, charge distribution, ECoN, Kutná Hora
Received: 26 April 2021; accepted: 15 October 2021; handling editor: J. Plášil
The online version of this article (doi: 10.3190/jgeosci.329) contains supplementary electronic material.

1. Introduction

The mineral vikingite was discovered among lillianite homologues from Ivigtut, Greenland, and described by Makovicky and Karup-Moller (1977b). Vikingite is a lillianite homologue with a homologue order number equal to 5.5, which is the average of the number of octahedra in two neighboring slabs separated by Pb atoms in trigonal prismatic coordination. In vikingite, there are 4 and 7 octahedra in two adjacent slabs. The value of the average N can be established without a structural analysis solely from the results of electron microprobe chemical analyses on the basis of equations given by Makovicky and Karup-Moller (1977a). In nature, vikingite can have various degrees of the lillianite substitution 2 Pb = Bi + Ag, usually from L% = 45 to 75%. The formula $Ag_5Pb_8Bi_{13}S_{30}$ for vikingite from the type locality Ivigtut, given by Makovicky and Karup-Moller (1977b), corresponds to $Vik_{71.5}$. The structure of vikingite was solved by Makovicky et al. (1992) on a sample from La Roche Balue, France, with the composition corresponding to Vik_{50}. However, it was unknown how the structure behaves with decreasing lillianite substitution under 50%, *i.e.*, with increasing Pb content accompanied by decreasing Ag and Bi contents. Also, the structure of Vik_{50} displayed some discrepancies, reflected in the differences between the ideal chemical formula for Vik_{50} and the formula established from the refinement (chemical formula $Ag_4Pb_{10}Bi_{12}S_{30}$ versus structural formula $Ag_{3.5.}Pb_{11.0}Bi_{11.5}S_{30}$).

In the Kutná Hora ore district, lillianite homologues were described by Pažout (2017) and the entire Bi-mineralization by Pažout et al. (2017). Typical for Kutná Hora and unique on a world scale is the presence of antimony in otherwise pure Ag–Pb–Bi sulfosalts. For lillianite homologues with N = 4, the Sb for Bi substitution was found to be nearly complete from almost pure

Sb members through transition members with *ca.* 50 : 50 ratio of Bi : Sb, such as staročeskéite (Pažout and Dušek 2010; Pažout and Sejkora 2018) to Sb-rich gustavite (Pažout and Dušek 2009), later described from Julcani, Peru, as a new mineral terrywallaceite (Yang et al. 2013) and to pure Bi members (gustavite with no Sb). Lillianite homologues with N > 4 from Kutná Hora (vikingite – $^{5.5}$L, treasurite – ^{6}L, eskimoite – ^{7}L, heyrovskýite – ^{7}L, erzwiesite – ^{8}L) also exhibit some contents of antimony which are unique and not known from other localities throughout the world. The Sb for Bi substitution is less pronounced than in N = 4 members with a general trend of decreasing Sb content with higher N. Thus, vikingite with N = 5.5 was found to have the Bi/(Bi + Sb) ratio as much as 0.75 (7.21 wt. % of Sb), while erzwiesite with N = 8 has a maximum Sb content equal to 0.89 (2.96 wt. % of Sb). The compositions of vikingite from the Staročeské pásmo Lode of Kutná Hora ore district varies: N = 5.17–5.75, Bi/(Bi + Sb) = 0.75–0.95. The sample for single-crystal analysis used in this study has this ratio equal to 0.89. The substitution percentage L % for vikingite from Kutná Hora ranges from 37 % (corresponding to $Ag_{2.6}Pb_{12.8}Bi_{10.6}S_{30}$) to 85 % (corresponding to $Ag_6Pb_6Bi_{14}S_{30}$). For the crystal structure study, the compositions close to end members are the most interesting. Therefore the vikingite grain used in this study was a good example of the low-end of the lillianite substitution, another reason being the Sb content.

The aim of this study was to determine the site populations of metal sites with regard to the two substitutions which take place in lillianite homologues in Kutná Hora ore district: 1) "lillianite" substitution 2 $Pb^{2+} = Ag^{+} + Bi^{3+}$ and 2) $Sb^{3+} = Bi^{3+}$. The study aims to establish which sites are filled and with what atoms with decreasing content of Ag and Bi and increasing Pb and whether antimony substitutes only for bismuth or also for lead.

2. Sample

The fragment of vikingite investigated by single-crystal X-ray diffraction was recovered from a specimen found by the first author on medieval mine dumps of Staročeské pásmo Lode of the Kutná Hora ore district, Czech Republic. The sample was extracted from a specimen of quartz gangue (ST 187) with fairly rich accumulations of silver grey metallic grains and crystal aggregates of several millimeters in size, consisting of Ag–Pb–Bi–Sb sulfosalts of lillianite homologous series, accompanied by Bi-rich jamesonite (Pažout 2020). Vikingite forms grey metallic grains associated with gustavite $Gus_{84\text{-}88}$ with Bi/(Bi + Sb) = 0.80 and izoklakeite with Bi/(Bi + Sb) = 0.63–0.70 (Fig. 1). Patches of parallel lamellation in Fig. 1 are formed by darker and brighter lamellae of Sb-rich gustavite (Bi/(Bi + Sb) > 0.75) which differ in L % (brighter lamellae have lower L % resulting in higher Pb and lower Ag + Bi). When the Sb content rises even more and the ratio Bi/(Bi + Sb) drops below ≤ 0.75, the lamellae-forming mineral becomes terrywallaceite (Yang et al. 2013) and again, the darker and brighter lamellae differ only in L %.

Microprobe data are in Tab. 1. The entire composition range of the vikingite grain, out of which the fragment for single-crystal analysis was extracted (Fig. 1), is $Vik_{37.5\text{-}45.9}$, N is between 5.17 and 5.71 and Bi/(Bi + Sb) is 0.88–0.89, corresponding to 2.22–2.84 wt. % of Sb.

Tab. 1 Chemical compositions of the Sb-rich vikingite grain (Fig. 1), from which the fragment for single-crystal X-ray analysis was extracted (wt. % and empirical formula coefficients, *apfu*).

	1	2	3	4	5	mean
Ag	5.02	4.80	5.54	5.23	5.62	5.24
Cu	0.00	0.01	0.01	0.03	0.03	0.02
Pb	43.14	43.94	39.70	40.06	40.22	41.41
Fe	0.02	0.04	0.03	0.02	0.03	0.03
Bi	32.64	32.33	35.47	34.71	34.85	34.00
Sb	2.31	2.22	2.84	2.74	2.61	2.54
S	16.15	16.00	16.20	16.30	16.09	16.15
Total	99.26	99.32	99.78	99.08	99.45	99.38
CH	–2.0	–1.0	0.5	–1.6	0.3	
apfu	56	56	56	56	56	
Ag	2.79	2.68	3.05	2.89	3.11	2.90
Cu	0.00	0.01	0.01	0.03	0.03	0.01
Pb	12.49	12.78	11.39	11.52	11.60	11.96
Fe	0.02	0.04	0.04	0.02	0.03	0.03
Bi	9.36	9.32	10.09	9.90	9.96	9.73
Sb	1.14	1.10	1.39	1.34	1.28	1.25
S	30.20	30.07	30.04	30.30	29.99	30.12
N	5.69	5.71	5.17	5.17	5.43	5.43
L %	39.22	37.50	45.87	44.11	45.36	42.41
x	0.72	0.69	0.73	0.70	0.78	0.72
Bi/(Bi + Sb)	0.89	0.89	0.88	0.88	0.89	0.89

CH – charge balance; N – order of lillianite homolog (Makovicky and Karup-Møller 1977); L % – percentage of the lillianite substiuion 2 $Pb^{2+} = Ag^{+} + (Bi,Sb)^{3+}$; *x* – substitution coefficient

3. Single-crystal X-ray crystallography

A tiny fragment of vikingite with dimensions of 0.184 × 0.066 × 0.039 mm was extracted from a polished sec-

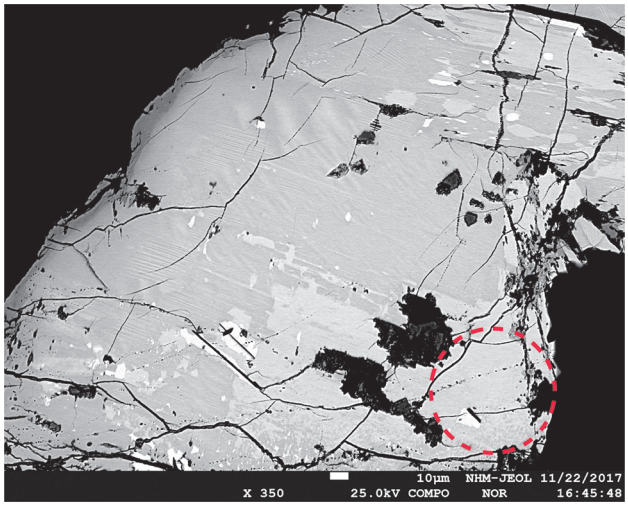

Fig. 1 BSE image of sample ST 187 with prevalent darker gustavite $Gus_{84–88}$ and izoklakeite. The fragment of vikingite Vik_{40} for single-crystal analysis was extracted from the vikingite grain with the composition $Vik_{37–46}$, marked by the circle. The diameter of the orange circle is 70 μm.

tion of sample ST 187 and separated under the optical stereomicroscope. The intensity data were collected using an Oxford Diffraction SuperNova single-crystal diffractometer equipped with an Atlas S2 CCD detector and monochromated Mo*K*α radiation (55 kV, 30 mA) focused by the mirrors. The unit-cell parameters were refined by a least-squares algorithm using the CrysAlis Pro Package (Rigaku 2019) from 2140 reflections and gave $a = 13.5394(10)$, $b = 4.0992(3)$, $c = 25.506(3)$ Å, $\beta = 95.597(8)°$ with $V = 1408.9(2)$ Å^3 and $Z = 1$, space group $C2/m$. From the total of 10503 measured reflections, 7441 were classified as observed [$I_{obs} > 3\sigma(I)$]. After averaging, 2049 reflections were independent and 1627 were classified as observed. Data were corrected for background, Lorentz and polarization effects, and an absorption correction based on the crystal shape (gaussian approach), followed by a multi-scan correction based on spherical harmonic functions, resulting in R_{int} of the merged data equal to 0.0692.

The crystal structure was solved from X-ray diffraction data by the charge-flipping algorithm (Palatinus and Chapuis 2007), independently from the previous structure solution (Makovicky et al. 1992). The obtained model was refined by the full-matrix least-squares of the Jana2006 program (Petříček et al. 2014). All atomic positions were found from the structure solution. Atom numbering scheme used in this study is the same as in Makovicky et al. (1992). Because the dominant metal atoms in the structure are lead and bismuth, undistinguishable by X-ray diffraction (but distinguishable by bond lengths, bond valences and charge density distribution), it was helpful first to establish an estimate of the electron content (number of electrons) of each metal site concerning heavy atoms content (Pb^{2+}, Bi^{3+}) *versus* lighter metal atoms content (Ag^{+}, Sb^{3+}). To this end, all metal atoms were assumed to be bismuth and their occupancies refined with isotropic displacement parameters. The refinement showed that the electron content of the marginal site *Me*4 of thicker ^{7}L slabs is lower than that of marginal site *Me*2 of ^{4}L slabs (i.e., *Me*4 contains more Ag than *Me*2), unlike the structure of Vik_{50} where *Me*4 has less Ag than *Me*2. However, X-ray data were not very sensitive to changes in the chemical composition of individual sites. As a result, the chemical changes in different structural models were not efficiently reflected in a change of *R* factors or residual electron density. Eventually, the program ECoN21 (Ilinca, pers. comm.) for calculation of charge distributions (CD), elaborated in papers of Hoppe et al. (1989) and Nespolo (2016), proved to be the most effective tool to check the correctness of each refined structural model, with emphasis on the comparison and match between oxidation numbers of cations q_X (corrected for site occupancy factors – *sof*) and anions q_A with charges received by cations $\mathbf{Q_X}$, and anions $\mathbf{Q_A}$ of each site in each structural model. The program calculates various parameters, including weighted average bond lengths, effective coordination numbers of each polyhedron, charges received by cations *versus* oxidation numbers of cations and bond valence sums. Similar to the approach of first estimating the electron content of each metal site from X-ray data by refining occupancies of all atoms set to Bi, a method of "bracketing" can be applied for the calculations in ECoN21. This meant that the charge distributions of all atoms in an initial refined structural model were calculated in ECoN21 and in the next step, a completely reversed configuration was applied, i.e., Bi atoms were replaced by Pb atoms, Pb atoms by Bi atoms and Ag–Bi sites by Ag–Pb sites. The new model was refined and subsequently calculated in ECoN21 and the charge distribution of all sites was compared to the reversed model. The calculations in ECoN21 showed several things that would be difficult to reveal from X-ray data only: 1. the mixed sites *Me*2 and *Me*4 are not composed of just Bi and Ag, but also contain Pb; 2. the central site *Me*1 in ^{4}L slabs is not Bi (or Bi with minor Ag), but a Bi–Pb mixed site; 3. the site *Me*6 is not a pure Pb site but contains some Bi.

In the Ag–Bi–Pb sites *Me*2 and *Me*4, the Pb content could be refined against Ag with the Bi occupancy fixed at 0.50 (as estimated from ECoN21), the sum of the site occupancies of all three atoms kept at unity and the coordinates and atomic displacement parameters (*ADPs)* of all three atoms kept identical. Finally, the anisotropic displacement parameters of all metal atoms were refined. An inspection of the refinement listing revealed a possible problem with nonmatching reflections. Because X-ray data from fragments of sulfosalts extracted from polished sections are rarely perfect (and especially those

Tab. 2 Crystallographic data and refinement details for Sb-rich vikingite from Kutná Hora. Czech Republic.

Crystal data	
Structure formula	$Ag_{2.85}Pb_{12.35}(Bi_{9.52}Sb_{1.27})_{\Sigma 10.80}S_{30}$
Crystal system	monoclinic
Space group	*C*2/*m*
Unit-cell parameters: *a*, *b*,*c* [Å]	13.5394(10), 4.0992(3), 25.506(3)
β [°]	95.597(8)
Unit-cell volume [Å3]	1408.9(2)
Z	1
Calculated density [g/cm3]	7.0412
Crystal size [mm]	0.184 × 0.066 × 0.039
F_{000}	2482
Data collection	
Diffractometer	Oxford Diffraction SuperNova, Atlas detector
Temperature [K]	284
Radiation. wavelength [Å]	MoK_α, 0.71073 (50 kV, 30 mA)
θ range for data collection [º]	3.02−29.57
Limiting Miller indices	$h = -18 \rightarrow 18$, $k = -5 \rightarrow 5$, $l = -35 \rightarrow 33$
Axis, frame width (º), time per frame (s)	ω, 1, 65
Total reflections collected	10503
Observed reflections, criterion	7441, [$I > 3\sigma(I)$]
Absorption coefficient [mm^{-1}]; type	69.04; gaussian
T_{min}/T_{max}	0.019/0.139
R_{int}	0.0692
Structure refinement by Jana2006	Full-matrix least-squares on *F*
Refined parameters, restraints, constraints	66, 0, 48
R, wR (obs)	8.60, 7.83
R,wR (all)	12.82, 8.73
GOF obs/all	2.34, 2.09
Weighting scheme, weights	σ, $w = 1/(\sigma^2(I)+0.0001I^2)$
Largest diffraction peak and hole (e Å^{-3})	7.67,–8.94

Tab. 3 Atom coordinates and displacement parameters for the crystal structure of Bi-rich vikingite from Kutná Hora, Czech Republic.

Atom	Occupancy	*x/a*	*y/b*	*z/c*	U_{eq}
*Me*1	Bi 0.54	0.12910(5)	0.5	0.96118(3)	0.0148(2)
	Sb 0.06	0.12910(5)	0.5	0.96118(3)	0.0148(2)
	Pb 0.40	0.12910(5)	0.5	0.96118(3)	0.0148(2)
*Me*2	Bi 0.50	0.39275(6)	0.5	0.89496(4)	0.0233(3)
	Pb 0.214(7)	0.39275(6)	0.5	0.89496(4)	0.0233(3)
	Ag 0.286(7)	0.39275(6)	0.5	0.89496(4)	0.0233(3)
*Me*3	Pb 1.0	0.14505(6)	0	0.80680(5)	0.0403(4)
*Me*4	Bi 0.50	0.36003(7)	0.5	0.71343(4)	0.0267(4)
	Pb 0.074(8)	0.36003(7)	0.5	0.71343(4)	0.0267(4)
	Ag 0.426(8)	0.36003(7)	0.5	0.71343(4)	0.0267(4)
*Me*5	Bi 0.741(9)	0.57168(6)	0	0.64576(4)	0.0237(3)
	Sb 0.259(9)	0.57168(6)	0	0.64576(4)	0.0237(3)
*Me*6	Pb 0.90	0.28533(6)	0	0.57122(4)	0.0371(3)
	Bi 0.10	0.28533(6)	0	0.57122(4)	0.0371(3)
*Me*7	Pb 1.0	0.5	0.5	0.5	0.0389(5)
S1		0.5	0.5	0	0.128(6)
S2		0.2484(3)	0	0.92198(19)	0.0179(10)
S3		0.0202(3)	0.5	0.86723(17)	0.0100(9)
S4		0.2862(4)	0.5	0.8035(2)	0.0267(12)
S5		0.4958(4)	0	0.7342(2)	0.0248(12)
S6		0.6996(6)	0.5	0.6860(3)	0.065(2)
S7		0.4305(4)	0.5	0.6053(2)	0.0280(12)
S8		0.3501(4)	0	0.4696(2)	0.0297(13)

containing significant Pb and Bi or other metals with high absorption), it was necessary to exclude the outliers in groups of symmetrically equivalent reflections, and these not on the basis of their deviation from the average measured intensity, but on how they deviate from individual calculated structure factors. Therefore, unaveraged reflection data were used for the final cycles of refinement. A criterion of skipping non-matching reflections with $|F_{obs}-F_{calc}| > 5\sigma(F_{obs})$ was used. The final correct structural model was obtained using averaged intensity data (*i.e.*, in a standard manner) where the influence of nonmatching reflections is not so strong but shows in higher residual electron density. The correct composition obtained using averaged reflections indicates that the structural model is correct and can be used to identify bad (nonmatching) reflections in unaveraged intensity data. After removing these bad reflections, *i.e.*, by using the $|F_{obs}-F_{calc} > 5\sigma(F_{obs})$ cutoff, we have returned to the correct final structural model. Nevertheless, this time it was with a better residual electron density and better *R* factors.

Similar to the structure of vikingite Vik_{50} by Makovicky et al. (1992), anisotropic displacement parameters (ADP) were refined for metal sites, isotropic displacement parameters were used for sulfur. The rather large displacement parameters of *Me*3 and S1 point to the possibility that the two positions are slightly disordered. The final refinement converged to an $R_1 = 0.0860$, $wR_2 = 0.0783$ with a GOF = 2.09 for 8500 measured reflections. Details of the data collection and the crystallographic and structure

refinement parameters are listed in Tab. 2. The final atom coordinates, occupancies and isotropic displacement parameters are given in Tab. 3 and the anisotropic displacement parameters are given in Tab. 4. The interatomic distances in Sb-rich vikingite Vik_{40} and comparison with equivalent distances in vikingite Vik_{50} are in Tab. 5. The detailed results of charge distribution calculations of metal and sulfur sites in the structure of Sb-rich vikingite Vik_{40} by program ECoN21 are in Tab. 6. The comparison of refinement results on using different cutoffs of nonmatching reflections is in Tab. 7. The table shows potential problems may include high residual electron density, negative values of occupancies, negative atomic displacement parameters, or structural formula deviating too much from the chemical analysis. The CIF file, also containing a block with the reflections, is provided as a Supplementary file at the Journal's web page www.jgeosci.org.

Tab. 4 Anisotropic displacement parameters (in Å^2) for the crystal structure of Sb-rich vikingite from Kutná Hora, Czech Republic.

Atom	U_{11}	U_{22}	U_{33}	U_{12}	U_{13}	U_{23}
*Me*1	0.0032(3)	0.0029(4)	0.0383(5)	0	0.0019(3)	0
*Me*2	0.0193(5)	0.0129(6)	0.0380(7)	0	0.0044(4)	0
*Me*3	0.0205(4)	0.0081(5)	0.0909(8)	0	–0.0019(5)	0
*Me*4	0.0231(6)	0.0131(6)	0.0444(8)	0	0.0050(5)	0
*Me*5	0.0221(5)	0.0136(5)	0.0354(6)	0	0.0029(4)	0
*Me*6	0.0307(5)	0.0275(6)	0.0534(7)	0	0.0052(4)	0
*Me*7	0.0438(8)	0.0291(8)	0.0428(8)	0	–0.0019(7)	0

4. Results

The crystal structure of vikingite contains fifteen independent sites, eight of them occupied by S and seven metal sites (Fig. 2). Of these, two are pure Pb sites (*Me*3 and *Me*7), two are Ag-Bi-Pb sites (*Me*2 and *Me*4), two are Pb-Bi sites (*Me*6 and *Me*1 with minor Sb) and one is Bi-Sb site (*Me*5). All sites except for *Me*3 are in distorted octahedral coordination.

The structure of vikingite is composed of thinner slabs (^{4}L) of four octahedra *Me*2–*Me*1–*Me*1–*Me*2 and thicker slabs (^{7}L) of seven octahedra *Me*4–*Me*5–*Me*6–*Me*7–*Me*6–*Me*5–*Me*4 separated by Pb atoms *Me*3 in trigonal prismatic coordination. The arrangement of ^{4}L and ^{7}L slabs in the crystal structure of vikingite is in Fig. 3.

The bicapped trigonal prism *Me*3, separating the ^{4}L and ^{7}L slabs and surrounded by *Me*2 and *Me*4 octahedra, is one of the least distorted polyhedra in the structure (together with *Me*7), with an effective coordination number *ECoN* = 6.91, a value close to ideal 7, and is thus even less distorted than the same prism in Vik_{50} (*ECoN* = 6.87). The site is occupied solely by Pb, as in all lillianite homologues with L % ≤ 100. The weighted average bond length R_{AV} is similar in both structures, 3.037 Å in Vik_{40}, 3.045 Å in Vik_{50}. The influence of Ag + Bi for Pb substitution on the position of S atoms which cap the vertical faces of the prism (S2 and S6), has not been confirmed in the current study. This influence, reported by Makovicky et al. (1992) in the structure of Vik_{50}, showed a shortening of these distances with more pronounced Ag–Bi substitution (higher Ag content). In $Vik_{50,}$ the *Me*3–S2 distance of 3.13 Å and *Me*3–S6 distance of 3.29 Å are in agreement with the more pronounced Ag + Bi substitution in the *Me*2 site (0.48 Ag + 0.52 Bi) adjacent to S2 in the ^{4}L slabs and with the less pronounced substitution in *Me*4 (0.38 Ag + 0.62 Bi) adjacent to S6 in the ^{7}L slabs (Makovicky et al. 1992). However, in vikingite $Vik_{40,}$ the distances are very similar (*Me*3–S2 distance of 3.13 Å and *Me*3–S6 distance of 3.24 Å) although the

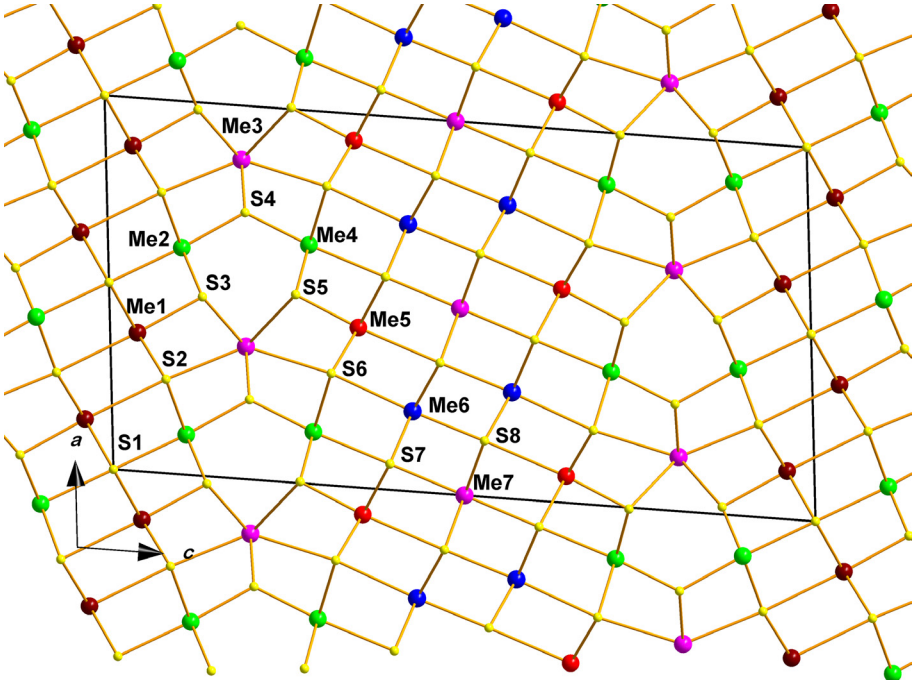

Fig. 2 Atom labelling in the crystal structure of vikingite. The atom numbering scheme is the same as in the structure of vikingite by Makovicky et al. (1992).

Tab. 5 Interatomic distances in Sb-rich vikingite Vik_{40} (this paper, left column) and in the structure of vikingite Vik_{50} (Makovicky et al. 1992, right column).

Sb-rich vikingite Vik_{40}			vikingite Vik_{50} (1992)		
*Me*1	S3	2.6884(3)	*Me*1	S3	2.5818
	S2	2.8503(2)		S2	2.7775
	S2	2.8505(2)		S2	2.7777
	S1	2.9280(2)		S1	2.9440
	S1	2.9281(2)		S1	2.9441
	S2	3.2655(4)		S2	3.2238
	R_{AV}	2.857		R_{AV}	2.788
*Me*2	S4	2.6205(3)	*Me*2	S4	2.5253
	S3	2.8128(2)		S3	2.7556
	S3	2.8130(2)		S3	2.7558
	S1	2.9200(3)		S1	2.9231
	S2	2.9595(2)		S2	3.1001
	S2	2.9597(2)		S2	3.1003
	R_{AV}	2.816		R_{AV}	2.758
*Me*3	S4	2.8086(1)	*Me*3	S4	2.8064
	S4	2.8087(1)		S4	2.8065
	S2	3.1296(4)		S2	3.1260
	S3	3.1540(2)		S3	3.2278
	S3	3.1542(2)		S3	3.2280
	S6	3.2379(4)		S5	3.2582
	S5	3.3132(2)		S5	3.2583
	S5	3.3134(2)		S6	3.2883
	R_{AV}	3.037		R_{AV}	3.045
*Me*4	S4	2.5941(3)	*Me*4	S4	2.5434
	S5	2.7697(1)		S5	2.7562
	S5	2.7698(1)		S5	2.7563
	S7	3.0055(3)		S7	2.9543
	S6	3.0185(2)		S6	3.0656
	S6	3.0187(2)		S6	3.0657
	R_{AV}	2.801		R_{AV}	2.771
*Me*5	S5	2.5677(3)	*Me*5	S5	2.6067
	S6	2.8122(2)		S6	2.8075
	S6	2.8124(2)		S6	2.8077
	S7	2.9215(2)		S7	2.9418
	S7	2.9216(2)		S7	2.9419
	S8	3.2216(4)		S8	3.1525
	R_{AV}	2.793		R_{AV}	2.814
*Me*6	S8	2.8177(3)	*Me*6	S8	2.9221
	S8	2.8763(2)		S8	2.9222
	S8	2.8765(2)		S8	2.9435
	S7	2.9126(2)		S7	2.9351
	S7	2.9127(2)		S7	2.9352
	S6	3.2517(4)		S6	3.0598
	R_{AV}	2.902		R_{AV}	2.948
*Me*7	S7	2.9308(3)	*Me*7	S7	2.9840
	S7	2.9311(3)		S7	2.9849
	S8	2.9351(2)		S8	2.9053
	S8	2.9353(2)		S8	2.9055
	S8	2.9353(2)		S8	2.9060
	S8	2.9355(2)		S8	2.9062
	R_{AV}	2.934		R_{AV}	2.929

R_{AV} – weighted average bond length calculated by ECoN 21 (Ilinca 2021, pers.comm.)

Ag–Bi substitution exhibits the opposite, as *Me*2 has only 28.6 % Ag and *Me*4 has 42.6 % Ag. This may be caused by the presence of lead in these sites, more pronounced in the *Me*2 position (see below). The bond lengths are typical of lead atoms in trigonal prismatic coordination in lillianite homologs.

All detectable Ag substitution occurs in the marginal octahedral sites *Me*2 and *Me*4 with typical short and long opposing distances, 2.62 and 2.92 Å for *Me*2 and 2.594 and 3.005 Å for *Me*4, more contrasting for the latter in line with a more pronounced Ag substitution in *Me*4. At the same time, the bond length ratio of the opposing short and long bonds of these sites is considerably less pronounced than in the case of Vik_{50} (2.525 and 3.100 Å) and (Ag, Bi)-bearing heyrovskýite Hey_{52} (2.479 and 3.043 Å, Makovicky et al. 1991), in agreement with the hybrid character of the triply substituted mixed sites in Vik_{40}.

*Me*4 is an octahedral site at the margin of the thicker ^{7}L slabs with the composition 0.426(8) Ag + 0.574 (Bi + Pb), very similar to the Bi3Ag3 site in synthetic orthorhombic N = 8 member (^{8,8}L) of the lillianite homologous series (Topa et al. 2010). Slightly larger values reflect the Pb content in this site in Vik_{40}. Charge distribution results from ECoN21 suggested a small amount of lead, eventually refined as 0.074(8) Pb. With the effective coordination number *ECoN* = 5.309, this octahedron is less distorted than *Me*4 in Vik_{50} which has 0.38 Ag + 0.62 (Bi + Pb) and *ECoN* = 5.053. The weighted average bond length R_{AV} of 2.801 Å is larger than that of Vik_{50} (2.771 Å, Tab. 5), reflecting both the lower Ag content and the presence of lead in this site in Vik_{40}.

*Me*2 represents a marginal octahedral site in the thinner ^{4}L slabs. In contrast to Vik_{50}, the occupancy of Ag is lower, refined as 0.286(7) Ag + 0.214(7) Pb + 0.50 Bi. So the depletion of Ag and Bi, which is related to the decrease of L %, shows most profoundly in this marginal site of thinner ^{4}L slabs. This is the biggest difference compared to Vik_{50} where this site is basically 0.5 Ag + 0.5 Bi. This is also reflected in the R_{AV} value of 2.816 Å in Vik_{40}, which is significantly larger than 2.758 for Vik_{50}. With the effective coordination number *ECoN* = 5.632, this octahedron is much less distorted than *Me*2 in Vik_{50} which has 0.48 Ag + 0.52 Bi and *ECoN* = 4.902. The positional disorder of *Me*2 and *Me*4 is smaller (and similar to Vik_{50}), but the coordinated sulfur atom S1 displays high atomic displacement parameters.

With decreasing substitution and growing Pb content, the central site *Me*1 in the thinner ^{4}L slabs, a practically pure Bi site in Vik_{50} (0.97 Bi + 0.03 Ag), becomes a Bi–Pb site with minor Sb (0.54 Bi + 0.06 Sb + 0.40 Pb). The weighted average bond length R_{AV} of 2.816 Å is significantly larger than 2.758 Å in Vik_{50}; the average of the three shortest bonds is 2.80 Å compared to 2.71 Å in Vik_{50}, evidencing a significant presence of lead in this

site in Vik_{40}. Charge distribution calculations also indicated that a small part of bismuth is substituted by antimony. The effective coordination number *ECoN* = 5.379. Thus this octahedron is less distorted than *Me*1 in Vik_{50}, which has *ECoN* = 5.101. The two opposing short and long distances perpendicular to the 4 Å *c* axis are 2.688 and 3.266 Å, suggesting a hybrid character caused by the mixing of lead and bismuth combined with antimony in this site.

The thicker ^{7}L slabs are formed, apart from the marginal octahedron *Me*4, by a semimarginal octahedral site *Me*5 and two central octahedra *Me*6 and *Me*7. The most central site *Me*7 is a pure Pb site in Vik_{40} and Vik_{50}, with similar weighted average bond lengths and effective coordination numbers. R_{AV} = 2.934 Å in Vik_{40} and 2.929 Å in Vik_{50} and *ECoN* = 6.000 and 5.968, respectively, which shows that this polyhedron is very symmetric and close to an ideal octahedron in both structures.

Tab. 6 Detailed results of charge distribution calculations of metal and sulfur sites in the structure of Sb-rich vikingite Vik_{40} in the cation-centered description by program ECoN 21 (Ilinca, pers. comm.).

Cation	sof	R_{AV}	ECoN	q_X	Q_X	q_X/Q_X	BVS
*Me*1	0.540 Bi, 0.060 Sb, 0.400 Pb	2.857	5.379	2.600	2.590	1.004	2.458
*Me*2	0.500 Bi, 0.214 Pb, 0.286 Ag	2.816	5.632	2.214	2.255	0.982	2.078
*Me*3	Pb	3.037	6.908	2.000	2.062	0.970	1.955
*Me*4	0.074 Pb, 0.500 Bi, 0.426 Ag	2.801	5.309	2.074	2.096	0.989	1.780
*Me*5	0.741 Bi, 0.259 Sb	2.793	5.131	3.000	3.006	0.998	2.795
*Me*6	0.900 Pb, 0.100 Bi	2.902	5.609	2.100	2.029	1.035	2.177
*Me*7	Pb	2.934	6.000	2.000	1.923	1.040	2.076
		MAPD(Q_X): 1.97 %			*MAPD(BVS)*: 6.05 %		

Anion	Bonding atoms	q_A	Q_A	q_A/Q_A
S1	*Me*1 4×, *Me*2 2 ×	–2.000	–2.264	0.883
S2	*Me*1 3×, *Me*2, *Me*3	–2.000	–1.914	1.045
S3	*Me*1, *Me*2 2×, *Me*3 2×	–2.000	–1.895	1.056
S4	*Me*2, *Me*3 2×, *Me*4	–2.000	–1.965	1.018
S5	*Me*3 2×, *Me*4 2×. *Me*5	–2.000	–1.993	1.003
S6	*Me*3, *Me*4 2×, *Me*5 2×, *Me*6	–2.000	–1.886	1.060
S7	*Me*4, *Me*5 2×, *Me*6 2×, *Me*7	–2.000	–2.156	0.928
S8	*Me*5, *Me*6 3×, *Me*7 2×	–2.000	–2.044	0.978
	MAPD(Q_A): 5.07%	*MAPD(BVS)*: 7.94 %		

Sof – site occupational factor
R_{AV} – Weighted average bond length
ECoN – Effective coordination number
Q_X – Charge received by cations
q_X – Oxidation number of cations
BVS – Bond valence sum
Q_A – Charge received by anions
q_A – Oxidation number of anions
MAPD – Mean absolute percentage deviation of Q_X, Q_A and *BVS*

A different situation is in the other central site *Me*6 (second from the center, third from the margin), which is a pure Pb site in Vik_{50}, but in Vik_{40}, with lower L%, higher Pb and lower Bi, this site becomes a Pb–Bi site with 10% of Bi, by paradox, as shown by charge-density calculations in ECoN21. Coordination-wise, this site is the least characteristic site as it has a long bond of 3.252 Å with the opposing too-long "short" bond of 2.818 Å, suggesting a positional/occupational disorder. The weighted average bond length R_{AV} of 2.902 Å is significantly shorter than 2.948 Å in Vik_{50}. The average of the three shortest bonds is 2.857 Å compared to 2.929 Å in Vik_{50}, showing this site is not a pure Pb site in Vik_{40}. This is also supported and reflected by the distortion of the polyhedron. The pure Pb site in Vik_{50} is much less distorted with *ECoN* = 5.949 while in Vik_{40} *ECoN* = 5.609. Pure octahedral Pb sites in sulfosalts usually show a very good match with the ideal coordination number 6.00 for the polyhedron.

The semimarginal site *Me*5, a pure Bi site in Vik50 with no Sb, was found to be the site where the Sb for Bi substitution occurs. It contains 0.741(9) Bi + 0.259(9) Sb. It is the most distorted site in the structure, probably due to the pronounced electron pair micelle, with *ECoN* = 5.131. The weighted average bond length R_{AV} of 2.793 Å is slightly shorter than 2.814 Å in Vik_{50} with no antimony content. The shortest bond *Me*5–S5 of 2.568 Å is considerably shorter than the equivalent shortest bond in Vik_{50} of 2.607 Å.

Tab. 7 The comparison of refinement results on using different cutoffs of nonmatching reflections.

X–ray data	All reflections	Excluded reflections	R_{obs}	wR_{obs}	GOF(all)	residual density (e Å^{-3}) peak	hole	sof	ADP	structure formula coefficients Ag	Pb	Bi	Sb
averaged	2049		16.33	19.12	7.76	18.91	–23.05	ok	S2 negative	2.88	12.32	9.49	1.31
unaveraged	10503	none	15.05	16.49	4.83	18.73	–21.88	ok	S2 negative	3.01	12.19	9.04	1.76
unavaraged cutoff 15	10315	188	13.75	13.95	4.01	15.69	–21.33	Pb4 0.032	ok	3.18	12.02	8.81	1.99
unaveraged cutoff 10	9933	570	12.12	11.73	3.35	13.70	–16.81	Pb4 0.16	ok	3.63	11.57	8.02	2.78
unaveraged cutoff 5	8500	2003	8.60	7.83	2.09	7.67	–8.94	ok	ok	2.85	12.36	9.52	1.28
									vikingite Vik_{40} *apfu* from EPMA	2.85	12.35	9.50	1.30

The average of the three shortest bonds does not differ that much: 2.731 Å in Vik_{40} and 2.741 in Vik_{50}. It is a mixed cation site with hybrid distances characteristic of mixed Bi–Sb positions with opposing distances of 2.568 and 3.222 Å and similar to Bi*2b* site in Sb-rich gustavite with almost the same Bi : Sb ratio (Pažout and Dušek 2009)

Generally speaking, sites in Vik_{50} (Makovicky et al. 1992) are more distorted than in Vik_{40} (this paper). The most distorted site in Vik_{50} is *Me*2 with *ECoN* = 4.902, followed by *Me*4 (*ECoN* = 5.053) and *Me*1 (*ECoN* = 5.101). In Vik_{40}, the most distorted sites are *Me*5, followed by *Me*4 and *Me*1. *Me*2, where the biggest change against Vik_{50} occurs in the form of considerably lower Ag content, is much less distorted, with *ECoN* similar to *Me*6 (Tab. 6).

The final structural formula is $Ag_{2.85}Pb_{12.35}(Bi_{9.52}Sb_{1.27})_{\Sigma=10.80}S_{30}$, corresponding to $Vik_{40.0}$, ideally $Ag_{2.80}Pb_{12.40}Bi_{10.80}S_{30}$, which is a very good fit between structure and chemistry. From the results of structure determination, the composition of the thinner ^{4}L slabs, together with its share of trigonal prismatic Pb and S4 sites, is $Ag_{0.572}Pb_{2.228}(Bi_{2.08}Sb_{0.12})_{\Sigma2.20}S_6$, which does not correspond to any composition on the gustavite–lillianite join. Nevertheless, the Pb content corresponds to Gus_{38}, which would, however, requires 0.38 *apfu* Ag and 2.38 *apfu* Bi, while we have 0.57 *apfu* Ag (0.20 more) and 2.20 *apfu* Bi (0.18 less). This composition is not electrically neutral like in Vik_{50}, the charge of cations is +11.628 and the charge of anions is –12. The composition of ^{7}L slabs is $Ag_{0.852}Pb_{3.948}(Bi_{2.682}Sb_{0.518})_{\Sigma3.20}S_9$. The Pb content corresponds to heyrovskýite with L % = 41 (Hey_{41}), which would require 1.025 *apfu* Ag and 3.025 *apfu* Bi while we have 0.852 *apfu* Ag (0.17 less) and 3.20 *apfu* Bi (0.175 more). The charge of cations in ^{7}L slabs is +18.348, the charge of anions is –18. Because the structure as a whole is neutral (overall charge balance is +59.952 against –60.000), the charge compensation is materialized within both kinds of slabs, *i.e.*, within the unit cell.

The last issue to discuss is the periodicity of vikingite. Very weak 8 Å levels in diffraction data of vikingite from Ivigtut, Greenland, were reported by Makovicky and Karup-Møller (1977b) and even weaker 8 Å levels in the material from La Roche Balue, France (Makovicky et al. 1992), on which the crystal structure of Vik_{50} was solved. They concluded that the ordering of Ag and Bi in marginal octahedral sites *Me*2 and *Me*4 causes twinning with the unit cell parameters for the true cell of the ordered vikingite structure calculated from the subcell dimensions as a = 7.07, b = 8.20, c = 25.12, β = 84.72°, the space group P–1.

However, in the material from Kutná Hora, Czech Republic, there were no signs or traces of 8 Å levels. This is apparently caused by formation conditions not favorable for the origin of an ordered structure. To sum up the experience from diffraction experiments on vikingite material from various localities, it is obvious that vikingite can have weak (or very weak) 8 Å levels on the one hand or no traces of this on the other hand. If we accept the fact that some of vikingites in nature are (more or less) ordered and have an 8 Å periodicity with triclinic P–1 symmetry and others have 4 Å periodicity with monoclinic $C2/m$ symmetry, then we can consider the 4 Å cell of the latter to be their true cell. Then it is a matter of discussion if both cases are still the mineral vikingite or we deal with two different minerals. However, there is an IMA rule saying that ordered and disordered varieties have the same mineral name.

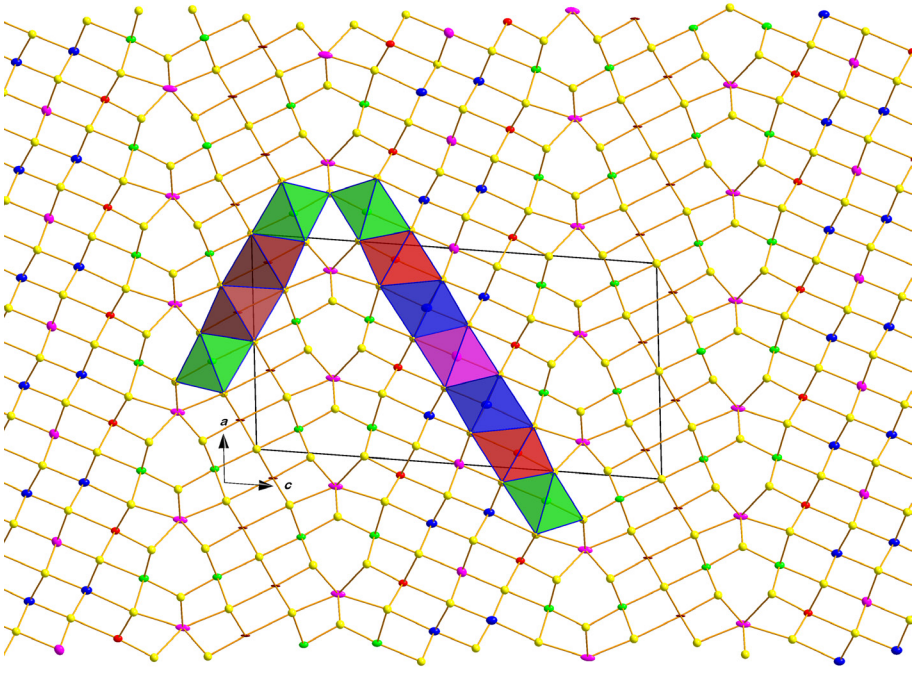

Fig. 3 General arrangement of ^{4}L and ^{7}L slabs in the crystal structure of vikingite. Chemical compositions of octahedral metal sites are differentiated by color: green (marginal octahedra *Me*2 and *Me*4): mixed Bi–Pb-Ag site; dark red (*Me*1 in the middle of ^{4}L slab): Pb-Bi mixed site with minor Sb; red (*Me*5): Bi–Sb site; blue (*Me*6): Pb–Bi mixed site; violet (*Me*7 in the center of ^{7}L slabs): pure Pb site and trigonal prismatic site *Me*3 that separates ^{4}L and ^{7}L slabs.

5. Conclusions

The comparison of the structures of vikingite Vik_{40} and Vik_{50} indicated how the decrease of the "lillianite" substitution $2\,Pb^{2+} = Ag^{+} + Bi^{3+}$ shows in site populations of metal sites. It was observed that up to 50 % of this substitution, the composition of marginal sites *Me*2 and *Me*4 is approximately 50 % Ag and 50 % Bi. When the L % decreases below 50 % (*i.e.*, Ag and Bi drop and Pb rises), the content of Ag begins to drop in one of the marginal sites below 50 % and simultaneously, this site is filled with lead. The content of Bi remains approximately 50 % even at this decrease. At the same time, the Ag content in the other marginal site decreases as well, but much more moderately. The site with the more substantial decrease in Ag content was identified to be *Me*2 of the thinner ^{4}L slabs.

Major changes against the previously published structure of Vik_{50} include:

1) Marginal octahedral sites *Me*2 and *Me*4, where the Ag–Bi substitution occurs, become Ag–Pb–Bi sites. The decrease of the 2Pb = Ag + Bi substitution below 50 % shows first in lowering of the Ag content of the marginal octahedral site *Me*2 in thinner ^{4}L slabs – which for vikingite with L % ≥ 50 is an *app.* fifty-fifty Ag–Bi site. The missing Ag is simultaneously replenished by Pb. At the same time, the occupancy of Ag in the marginal site *Me*4 in thicker ^{7}L slabs does not depart from 50 % so profoundly, 0.426 Ag + 0.574 (Bi + Pb).
2) The central *Me*1 site from ^{4}L slabs has no or minimal content of Ag. The central octahedron *Me*1 in thinner ^{4}L slabs, which is almost a pure Bi site in Vik_{50} (0.97 Bi + 0.3 Ag) becomes in Vik_{40} a Bi–Pb site with minor Sb (0.54 Bi + 0.06 Sb + 0.40 Pb).
3) Sb substitutes for bismuth. The Sb for Bi substitution takes place in semimarginal site *Me*5, refined as 0.741(9) Bi + 0.259(9) Sb. A small amount of antimony was detected in the Bi–Pb site *Me*1. The substitution of Sb for lead could not be confirmed.
4) The central octahedron *Me*6, a pure Pb site in Vik_{50}, becomes a Pb–Bi site with (0.9 Pb + 0.1 Bi).

Acknowledgments. This research was financially supported by the Czech Science Foundation (GAČR project 15-18917S). Dan Topa (Naturhistorisches Museum Wien) is thanked for his substantial help with grain extraction, polished section preparation and EPMA measurement. Crucial was the help of Gyuri Ilinca (University of Bucharest) with the program ECoN21. We thank Emil Makovicky for a constructive review and Jakub K. Plášil for a thoughtful review and editorial assistance.

Electronic supplementary material. Supplementary material consisting of crystal structure data for vikingite (cif) is available online at the Journal website (*http://dx.doi.org/10.3190/ jgeosci.329*).

References

Hoppe R, Voigt S, Glaum H, Kissel J, Müller HP, Bernet K (1989) A new route to charge distributions in ionic solids. J Less-Common Met 156: 105–122

Ilinca G (2021) ECoN21 a computer program for calculating charge distributions and bond valence sums in crystal structures. https://unibuc.ro/user/gheorghe.ilinca/?profiletab= documents

Makovicky E, Karup-Møller S (1977a) Chemistry and crystallography of the lillianite homologous series, part I. General properties and definitions. Neu Jb Mineral, Abh 130: 265–287

Makovicky E, Karup-Møller S (1977b) Chemistry and crystallography of the lillianite homologous series, part II. Definition of new minerals: eskimoite, vikingite, ourayite and treasurite. Redefinition of schirmerite and new data on the lillianite–gustavite solid solution series. Neu Jb Mineral, Abh 131: 56–82

Makovicky E, Mumme WG, Hoskins BF (1991) The crystal structure of Ag–Bi-bearing heyrovskyite. Canad Mineral 29: 553–559

Makovicky E, Mumme WG, Madsen IC (1992) The crystal structure of vikingite. Neu Jb Mineral, Mh 10: 454–468

Nespolo M (2016) Charge distribution as a tool to investigate structural details. IV. A new route to heteroligand polyhedra. Acta Crystallogr, Sect B 72: 51–66

Palatinus L, Chapuis G (2007) Superflip – a computer program for the solution of crystal structures by charge flipping in arbitrary dimensions. J Appl Crystallogr 40: 451–456

Pažout R (2017) Lillianite homologues from Kutná Hora ore district, Czech Republic: a case of large-scale Sb for Bi substitution. J Geosci 62: 37–57

Pažout R (2020) Distribution of Bi in the crystal structure of Bi-rich jamensonite, $FePb_4(Sb_{5.48}Bi_{0.52})_{\Sigma=6}S_{14}$. J Geosci 65: 261–265

Pažout R, Dušek M (2009) Natural monoclinic $AgPb(Bi_2Sb)_3S_6$, Sb-rich gustavite. Acta Crystallogr, Sect C Cryst Struct 65: 77–80

Pažout R, Dušek M (2010) Crystal structure of natural orthorhombic $AgPbBi_{1.75}Sb_{1.25}S_6$, a lillianite homologue with N = 4; comparison with gustavite. Eur J Mineral 22: 741–750

Pažout R, Sejkora J (2018) Staročeskéite, $Ag_{0.70}Pb_{1.60}(Bi_{1.35}Sb_{1.35})\Sigma_{2.70}S_6$, from Kutná Hora, Czech Republic, a new member of lillianite homologous series. Mineral Mag 82: 993–1005

Pažout R, Sejkora J, Šrein V (2017) Bismuth and bismuth–antimony sulfosalts from Kutná Hora vein Ag–Pb–Zn ore district, Republic. J Geosci 62: 37–57

Petříček V, Dušek M, Palatinus L (2014) Crystallographic Computing System Jana2006: general features. Z Kristallogr 229: 345–352

Rigaku (2019) CrysAlis CCD and CrysAlis RED. Rigaku–Oxford Diffraction Ltd, Yarnton, Oxfordshire, UK

Topa D, Makovicky E, Schimper HJ, Dittrich H (2010) The crystal structure of a synthetic orthorhombic N = 8 member of the lillianite homologous series. Canad Mineral 48: 1127–1135

Yang H, Downs RT, Evans SH, Pinch WW (2013) Terrywallaceite, $AgPb(Sb,Bi)_3S_6$,isotypic with gustavite, a new mineral from Mina Herminia, Julcani Mining District, Huancavelica, Peru. Amer Miner 98: 1310–1314